Int. J. Solids Structures Vol. 22, No. 10, pp. 1083–1106, 1986
Printed in Great Britain.

0020-7683/86 $3.00 + .00
Pergamon Journals Ltd

SHEAR, SHAPE AND ORIENTATION EFFECTS IN TRANSFORMATION TOUGHENING

J. C. LAMBROPOULOS†
Division of Applied Sciences, Harvard University, Cambridge, MA 02138, U.S.A.

(*Received* 7 *September* 1984)

Abstract—The continuum mechanics is formulated for the inelastic behavior of a ceramic material containing particles of a second phase ceramic which undergo a martensitic phase transformation when a function of the macroscopic stress state attains a critical value. A constitutive law is derived which is applicable to such materials viewed as composites. The constitutive law is similar in structure to the incremental (or flow) theories of metal plasticity in that it is characterized by a yield function (relating the critical values of the components of the stress state), a loading criterion (specifying the condition for continued deformation) and a set of flow equations (relating the increments of inelastic strains to the macroscopic stress state). Explicit forms of the constitutive law are presented for the cases in which the second phase particles are either spheres or thin oblate spheroids. The inelastic constitutive law is used to predict the toughness enhancement measured in ceramics which are strengthened by second phase particles (usually ZrO_2) which undergo both dilatational and shear irreversible transformations in the presence of a macroscopic crack. The near-tip stress intensity factor is related to the applied stress intensity factor for stationary and growth macroscopic cracks. Toughening is associated with crack growth and is due to the wake of transformed particles which are left behind a growing crack. The results show the importance of accounting for both the shear and dilatational components of the transformation as well as the importance of orientation effects on the values of the toughness enhancement.

1. INTRODUCTION

Within the last ten years or so, a remarkable mechanism has been discovered according to which the fracture toughness of ceramic materials can be greatly enhanced: according to the transformation toughening mechanism, inclusions of zirconia (ZrO_2) within a matrix of another ceramic can be made to retain metastably their tetragonal crystal structure down to room temperature and to transform irreversibly to monoclinic only in the presence of the high stresses near the tip of a macroscopic crack[1]. The transformation alters the stress distribution near the crack tip by decreasing the net near-tip stress intensity factor and the toughness of the material is thus greatly enhanced[2–5].

An important aspect of the transformation of ZrO_2 particles from tetragonal to monoclinic is the size effect[6, 7]. If the particles are too small, they do not transform to monoclinic in the presence of a macroscopic crack. When the particles are too large, they transform to monoclinic during fabrication and they are not available for the tetragonal to monoclinic transformation in the presence of a crack. Hence, in either case, the toughening effect due to the transformation is lost, although not entirely[8]. Furthermore, the transformation from tetragonal to monoclinic is martensitic[1] and, as such, it has drawn considerable attention[9].

According to whether the ZrO_2 particles are unconstrained or constrained by a surrounding matrix, the final morphology of the monoclinic particles varies. When unconstrained, a single crystal of tetragonal ZrO_2 transforms spontaneously to the monoclinic crystal structure. The unconstrained transformation is accomplished by a volume expansion of 3–5% and a shear of about 16%[10].

When the ZrO_2 particles are constrained by the surrounding matrix, they can be made to retain their tetragonal crystal structure if they are of the proper size and when the ceramic has been partially stabilized by alloying with Y_2O_3, MgO or CaO. Optimum microstructures are those that contain a homogeneous distribution of coherent tetragonal ZrO_2 particles[11]. The ZrO_2 particles are spherical when found in a matrix of Al_2O_3, or thin oblate spheroids

† Present address: Department of Mechanical Engineering, University of Rochester, Rochester, NY 14627, U.S.A.

when found in partially stabilized zirconia (PSZ). In PSZ the ZrO_2 particles usually arrange themselves in three mutually orthogonal directions[12]. When the ceramic is stressed sufficiently, the ZrO_2 particles transform to monoclinic by twinning which occurs in order to relieve the large shear component of the strain energy that would accumulate if twinning had not taken place. However, in addition to the volumetric transformation straining which is still 3–5% on the average over the particle, it is possible to have either short or long range shear transformation strains, i.e. the twinning may be such that the average shear transformation strain over the volume of the particle vanishes or does not vanish, respectively.

McMeeking and Evans[13] took into account only the dilatant part of the transformation and predicted increases in toughness which were in the same range as (but underestimated) the experimental data. Furthermore, Budiansky *et al.*[14] proposed a nonlinear mean stress-dilatation relation for the composite which allowed for unloading or loading in parallel to the classical theory of incremental plasticity. The advantage of the approach of Budiansky *et al.* was that it overcame the difficulty of accounting for microstructural details by postulating a relevant phenomenological description for the composite. Since only dilatational effects were taken into account, the shape of the transforming particles was irrelevant in the work of McMeeking and Evans[13] or Budiansky *et al.*[14].

In the present paper we propose a constitutive relation in the same vein as Budiansky *et al.*[14]. The constitutive law, presented in Section 2, takes into account both the volumetric and shear components of the transformation strain, as well as the shape and orientation of the transformed particles. The constitutive law is valid for systems with sufficiently small particles and spacing between particles such that the transformation zone at the crack tip includes many particles. Thus, a continuum description of the composite system can be developed.

Section 4 applies the proposed constitutive relation to the evaluation of the enhancement in the stress intensity factor (SIF) for a stationary crack and it is shown that greatly enhanced toughness cannot be attributed to the transformation zone at the tip of a stationary crack. Section 5 contains the calculation of the toughness enhancement due to the transformed particles left behind in the wake of a crack tip that advances stably and quasi-statically. Finally, the maximum possible toughness is determined and compared to available experimental data.

2. CONSTITUTIVE LAW

In this section the goal is to replace the inhomogeneous composite by a homogeneous material characterized by a nonlinear constitutive relation. Thus, we consider a sample of material which is made of a linear elastic matrix and of particles which are characterized by the stress-free transformation strain ε_{ij}^T and have the same elastic moduli as the matrix. We assume that all particles have the same orientation and the same shape but possibly different sizes. Thus, we denote by a the size of a typical particle. To develop the constitutive law in the spirit of continuum mechanics, we further assume that the sample contains sufficiently many particles so that the volume concentration dc of particles with sizes between a and $a+da$ is given by

$$dc = g(a)\,da. \tag{1}$$

We imagine that the composite is loaded by average uniform stresses $\bar{\sigma}_{ij}$ while the volume concentration of particles that have actually transformed is c. The value of c is found by

$$c = \int_a^\infty g(\xi)\,d\xi, \tag{2}$$

where $g(\xi)$ is defined by eqn (1) and the order of the limits reflects the fact that the larger particles will transform before the smaller ones according to the size effect mentioned in the Introduction.

The average stresses $\bar{\sigma}_{ij}$ are related to the average matrix stresses σ_{ij}^M and to the stresses σ_{ij}^G within the particles by

$$\bar{\sigma}_{ij} = c\sigma_{ij}^G + (1-c)\sigma_{ij}^M. \tag{3}$$

The particle stresses σ_{ij}^G can be found by employing the classical Eshelby results[15]. Hence, the matrix stresses σ_{ij}^M can be expressed in terms of the average stresses $\bar{\sigma}_{ij}$, the volume concentration c of transformed particles and the transformation strain ε_{ij}^T. Thus, any formulation in terms of σ_{ij}^M is equivalent to another in terms of $\bar{\sigma}_{ij}$. It is found, however, that the use of σ_{ij}^M is more convenient at this stage.

The fact that a volume concentration c of the particles has transformed while the current matrix stress state is σ_{ij}^M is expressed by an equation of the form

$$F(\sigma_{ij}^M) = H(c). \tag{4}$$

This equation is called the critical transformation condition in analogy to the theory of plasticity. It will be shown in the sequel that the functions F and H are such that $H(c)$ is a monotonically increasing function of c, and, hence, the requirement that the loading must increase for the volume concentration of transformed particles to further increase is expressed by

$$\mathrm{d}F(\sigma_{ij}^M) > 0, \tag{5}$$

where d( ) signifies the increment of ( ). This equation is the criterion for continued transformation in analogy to the loading criterion of the theory of metal plasticity.

When eqn (5) is satisfied, the corresponding increment dc is found by considering the increment of eqn (4). dc gives rise to an accompanying increment $\mathrm{d}\varepsilon_{ij}^p$ of the inelastic strains which is porportional to dc, i.e.

$$\mathrm{d}\varepsilon_{ij}^p = g_{ij}(\sigma^M)\,\mathrm{d}c. \tag{6}$$

Equation (6) is referred to as the flow rule and it completes the description of the constitutive relation.

It must be noted that the right-hand side of eqn (4) can be identified with a yield stress as in plasticity theory where, although the yield stress can be related to the microstructure of the metal, it is standard practice to determine the yield stress by an independent tensile experiment. In the sequel it will be shown that the function $H(c)$ of eqn (4) can be related in principle to the microstructure of the material, but it is suggested that $H(c)$ should be determined by an independent experiment and by fitting eqn (4) to the relevant data. On the other hand, it can be also argued that such an experiment is extremely difficult to perform as the stresses necessary to induce the transformation from tetragonal to monoclinic in ZrO_2 particles are very high and as such can be found only near severe stress raisers such as crack tips.

To completely specify the constitutive law, the functions F and g_{ij} of eqns (4) and (6) respectively must be determined, i.e. we need a physical statement describing the conditions for transformation and the corresponding increments in the accompanying inelastic strains. This will be done by considering an isolated ellipsoidal particle of size a embedded coherently within a matrix of nontransforming linear elastic material which is loaded by the uniform stresses σ_{ij}^M. The elastic moduli of the particle are taken to be the same as of the matrix.

Let us imagine that when $\sigma_{ij}^M = 0$ the inclusion does not transform, but as σ_{ij}^M is raised to some critical level the inclusion transforms (transformation characterized by ε_{ij}^T) and does so in a way that allows the formation of the twinned structure discussed in the

Introduction. For the transformation to take place, it is necessary that the change ΔG in Gibbs free energy of the system (matrix and particle) be nonpositive, i.e.

$$\Delta G = \Delta G_{\text{crit}} \leqslant 0, \tag{7}$$

where ΔG is written as

$$\Delta G = \Delta E_{\text{mech}} + \Delta E_0. \tag{8}$$

It is obvious that eqn (7) does not describe fully the necessary and sufficient conditions for transformation. Since ΔG is the difference in free energy between the final (monoclinic) and initial (tetragonal) states, any statement such as eqn (7) neglects the kinetics of the transformation. A more proper treatment might be to consider the circumstances under which an initial monoclinic embryo within the tetragonal particle will spread unstably throughout the whole particle. However, we propose to use eqn (7) as a guideline in deriving the multiaxial stress dependence of the function F of eqn (4). The motivation for this assumption is that the primary dependence of ΔG on σ_{ij}^M enters through ΔE_{mech}, and this dependence can be determined using the basic work of Eshelby[15], as will be done below.

In eqn (7), ΔG_{crit} is the critical value that ΔG must attain for the transformation to be thermodynamically favorable. ΔG_{crit} may depend in general on the size a of the particle, on the temperature, as well as on the alloying content[5]. In eqn (8), ΔE_{mech} is the change in mechanical potential energy of the system (particle and matrix) when the particle transforms from tetragonal to monoclinic. A lucid description of ΔE_{mech} is given in the recent book by Mura[16]. Finally, ΔE_0 in eqn (8) denotes collectively several terms: the change in chemical energy; the change in surface energy which is attributed to two sources (surface energy changes in the interface between the particle and the matrix, and surface energy changes due to the interface between the twinned bands). Lastly, ΔE_0 contains the strain energy accumulated in the matrix due to the formation of the twins. Evans *et al.*[6] estimated this last contribution for a spherical particle with equispaced bands and showed that it is localized near the particle–matrix interface and does not depend on the stress σ_{ij}^M.

It can be noted that for an ellipsoidal particle with uniform transformation strain ε_{ij}^T which is embedded coherently within an infinite elastic matrix loaded remotely by σ_{ij}^M, the term ΔE_{mech} can be calculated exactly[15]. It is given by

$$\Delta E_{\text{mech}} = -V_p(\sigma_{ij}^M + \tfrac{1}{2}\sigma_{ij}^I)\varepsilon_{ij}^T, \tag{9}$$

where V_p is the volume of the particle and σ_{ij}^I is the stress in the particle due solely to ε_{ij}^T (i.e. in the absence of σ_{ij}^M) which is given by

$$\sigma_{ij}^I = L_{ijkl}(S_{klmn} - I_{klmn})\varepsilon_{mn}^T, \tag{10}$$

where **L** is the elastic stiffness tensor of both particle and matrix, **S** is Eshelby's tensor and **I** is the identity tensor. Finally, we note that the stress in the particle after transformation is

$$\sigma_{ij}^G = \sigma_{ij}^I + \sigma_{ij}^M. \tag{11}$$

When the expression for ΔE_{mech} from eqn (9) is substituted into eqn (8) and then into eqn (7), we find the critical transformation criterion to be

$$(\sigma_{ij}^M + \tfrac{1}{2}\sigma_{ij}^I)\varepsilon_{ij}^T = \frac{E_0 - \Delta G_{\text{crit}}}{V_p}. \tag{12}$$

Thus, for a suitably chosen ε_{ij}^T (possibly depending on σ_{ij}^M) we propose to relate the left-hand side of eqn (12) to the function $F(\sigma_{ij}^M)$ of eqn (4).

To complete the description of the transformation it is necessary also to model the creation of the twinned structure upon transformation and, hence, determine ε_{ij}^T in eqn (12). Microscopy reveals that the structure of the twins within the transformed particles is quite complicated[9, 17, 18]. Often more than one family of twins is observed and the thickness of the alternating bands is size dependent[17]. Although twinning relieves some of the shear component of the strain energy due to transformation, it appears that not all of the shear strain energy is annihilated by twinning[12]. On the other hand, twinning takes place along well-defined crystallographic directions on crystallographic planes. Although many of these twin systems have been identified[9, 12, 19], it is still not clear what systems are operative under what conditions. Hence, the question arises of how to account properly for twinning.

Twinning does not alter the volumetric component ε_{ii}^T (3–5%) of the transformation strain. Furthermore, we assume that there is a nonvanishing average deviatoric component e_{ij}^T in the transformation strain which we find by postulating the following. The location of the twinned variants within each family and the thickness ratios of the various bands adjust suitably upon transformation so that at the instant just after transformation the deviatoric component of stress within the particle has been reduced to zero, i.e.

$$s_{ij}^G = 0, \tag{13}$$

where

$$\begin{aligned} s_{ij} &= \sigma_{ij} - \sigma_m \delta_{ij}, \\ \sigma_m &= \tfrac{1}{3}\sigma_{ii}. \end{aligned} \tag{14}$$

Obviously eqn (13) neglects the directional character of twinning which may not be valid for smaller particles[17]. Equation (13) could only be rigorously correct if the particle had infinitely many twin systems and we expect, thus, that (13) should overestimate the effect of twinning. Finally, we observe that eqn (12) implies that at transformation the particle acts, in effect, like a liquid particle which cannot support any shearing load and which undergoes a uniform dilatation ε_{ii}^T.

When we substitute from eqns (10) and (11) into eqns (13) and (14) we get

$$(I_{ijkl} - S_{ijkl} + \tfrac{1}{3}\delta_{ij}S_{mmkl})e_{kl}^T = \frac{s_{ij}^M}{2G} + \tfrac{1}{3}\varepsilon_{pp}^T(S_{ijkk} - \tfrac{1}{3}\delta_{ij}S_{mmkk}),$$

where G is the shear modulus of the material (assumed isotropic) and e_{ij} is the strain deviator defined by

$$e_{ij} = \varepsilon_{ij} - \tfrac{1}{3}\varepsilon_{pp}\delta_{ij}.$$

The equations above can be solved for e_{ij}^T, thus yielding

$$e_{ij}^T = \Lambda_{ijkl}s_{kl}^M + K_{ij}\varepsilon_{mm}^T, \tag{15}$$

where the tensors Λ and $\mathbf{K}$ depend on the elastic moduli and on the shape of the particle. We reiterate that eqn (15) yields the average (over the particle) of the deviatoric transformation strain and is much smaller than the 16% stress-free shear strain that the particle would undergo if it were unconstrained.

In the remaining part of the section, we will illustrate how the use of eqns (15) and (12) leads to the stress dependence of the function F of eqn (4) for spherical particles. The form of F for thin oblate spheroidal particles is obtained similarly and is shown in the Appendix.

For spherical particles, eqn (15) reduces to

$$e_{ij}^T = \frac{s_{ij}^M}{2G(1-\beta)}, \qquad \beta = \frac{2}{15}\frac{4-5\nu}{1-\nu}, \tag{16}$$

whereas (10) gives

$$\sigma_m^I = -B(1-\alpha)\varepsilon_{ii}^T, \qquad \alpha = \frac{1}{3}\frac{1+\nu}{1-\nu}, \tag{17}$$

where B is the bulk modulus and ν is Poisson's ratio. Substituting from (16) and (17) into eqn (12) and dividing through by the quantity $B(\varepsilon_{ii}^T)^2$ we get

$$m\left(\frac{\sigma_e^M}{p_0}\right)^2 + \frac{\sigma_m^M}{p_0} = \frac{\Delta E_0 - \Delta G_{\text{crit}}}{V_p B(\varepsilon_{ii}^T)^2} + \tfrac{1}{2}(1-\alpha) \equiv P(a), \tag{18}$$

where

$$m = \frac{B}{6G(1-\beta)} = \frac{5}{3}\frac{1-\nu^2}{(1-2\nu)(7-5\nu)},$$

$$p_0 = B\varepsilon_{ii}^T,$$

$$\sigma_e^2 = \tfrac{3}{2}s_{ij}s_{ij}.$$

Thus, the left-hand side of (18) is identified with the function $F(\sigma_{ij}^M)$ for spherical particles

$$F(\sigma_{ij}^M) = m\left(\frac{\sigma_e^M}{p_0}\right)^2 + \frac{\sigma_m^M}{p_0}. \tag{19}$$

Finally, we incorporate the size effect by assuming that the dependence of $P(a)$ on the size a [eqn (18)] is such that

$$\frac{dP}{da} \leqslant 0. \tag{20}$$

The form of the function F for thin oblate spheroids is listed in the Appendix. In either case, we can write

$$F(\sigma_{ij}^M) = P(a) \tag{21}$$

as the critical condition for transformation.

Now we can return to our original problem in which we had considered a collection of similarly shaped and oriented ellipsoidal inclusions by interpreting the size a of eqn (21) as the size of the smallest particle that has transformed while the current stress state in the matrix is σ_{ij}^M. Equation (2) can be inverted to yield

$$a = a(c),$$

which, when substituted into eqn (21), yields

$$F(\sigma_{ij}^M) = H(c), \tag{4}$$

where we have denoted $H(c) \equiv P(a(c))$. Since $dc/da < 0$ and $dP/da \leqslant 0$ from eqns (2) and (20), respectively, we conclude that

$$\frac{dH}{dc} \geqslant 0 \tag{22}$$

as outlined in the discussion of eqn (4).

Supposing that σ_{ij}^M increases according to the criterion for continued deformation, eqn (5), the increment dc in the volume of transformed particles gives rise to the increment $d\varepsilon_{ij}^p$ in the inelastic strains according to

$$\begin{aligned} d\varepsilon_{ii}^p &= \varepsilon_{ii}^T dc, \\ de_{ij}^p &= e_{ij}^T dc, \end{aligned} \tag{23}$$

where the value of e_{ij}^T is provided in general by eqn (15). The specific form of e_{ij}^T for spherical or thin ablate spheroidal particles is given in eqn (16) and in the Appendix, respectively. Thus, the flow rule is completely established.

Although the flow rule was derived from first principles, it can be shown that the inelastic strain increments are parallel to the normal of the function $F(\sigma_{ij}^M)$ in σ_{ij}^M-space, i.e.

$$d\varepsilon_{ij}^p = R\frac{\partial F}{\partial \sigma_{ij}^M} dc,$$

where R is a constant of proportionality. Normality is not fortuitous: general arguments have been put forth by Rice[20], who showed that a transformation criterion such as eqn (7) with ΔG_{crit} independent of σ_{ij}^M must necessarily obey normality.

3. STRESS-INDUCED TRANSFORMATION NEAR A CRACK TIP

As stated in the previous section, the transformation of ZrO_2 particles constrained within a nontransforming ceramic matrix requires high stresses which can be found only near severe stress raisers such as cracks. Thus, we propose to study the effect of transformation near a crack tip. The results concerning the toughness enhancement are different for the cases of stationary or growing cracks. In this section we will discuss the formulation of the problem of correlating the nominal loads to the near-tip stresses irrespective of the stationary or growing nature of the crack. In the subsequent sections we will present the results of our analysis as they apply to stationary or growing cracks.

We consider the case of a macrocrack of length b within a specimen of material characterized by the constitutive law derived in the previous section. The specimen is loaded in mode I and we assume that plane strain conditions prevail near the crack tip. Because of the high stresses that develop in the neighborhood of the crack tip, the material near the crack tip undergoes the stress induced transformation discussed in the Introduction and as a result a region Ω develops near the tip within which the material is transformed. A typical dimension of such a transformed region is only a few microns in extent[12]. Thus, the height of the transformed zone Ω is small compared to any other relevant length scales. Under this "small scale transformation" condition, an asymptotic problem for a semi-infinite crack can be formulated as follows.

With the small scale transformation condition, the stresses remote from the crack tip

are given by

$$\sigma_{ij} = \frac{K_\infty}{\sqrt{(2\pi r)}} f_{ij}(\theta) \qquad (r \to \infty), \tag{24}$$

where K_∞ is the elastic stress intensity factor (SIF) which is determined for the actual geometry of a cracked specimen under a given load. K_∞ is referred to as the applied SIF: its critical value is what is determined in a standard fracture toughness test. Under the assumption of mode I plane strain, the functions $f_{ij}(\theta)$ are universal and they are defined so that $f_{22}(0) = 1$. Hence, on the line $\theta = 0$ the normal stress is given by

$$\sigma_{22} = \frac{K_\infty}{\sqrt{(2\pi r)}} \qquad (r \to \infty).$$

On the other hand, as the crack tip is approached asymptotically the material is fully transformed and responds to applied loads in an incrementally linear manner. Thus, as $r \to 0$ the stress field has the same spatial dependence as in eqn (24) but now, in general, the SIF is different, i.e.

$$\sigma_{ij} = \frac{K_{tip}}{\sqrt{(2\pi r)}} f_{ij}(\theta) \qquad (r \to 0). \tag{25}$$

It is assumed that K_{tip} is the parameter that governs the fracture process near the crack tip. When there is no transformation K_∞ equals K_{tip}; hence, it is the reduction from K_∞ to K_{tip} that determines the toughness enhancement due to transformation. We relate K_{tip} to K_∞ by writing

$$K_{tip} = K_\infty + \Delta K_{tip}, \tag{26}$$

where

$$\Delta K_{tip} = \iint_\Omega \mathrm{d}K_{tip}. \tag{27}$$

In eqn (27), Ω is the upper half of the transformed region and $\mathrm{d}K_{tip}$ is the enhancement in the SIF under plane strain mode I conditions due to two differential elements of area $\mathrm{d}A$ undergoing a transformation strain. The first is located at (r, β) with respect to the crack tip and it is characterized by the stress-free strains E^T_{11}, E^T_{22}, E^T_{12} whereas the second is located at $(r, -\beta)$ and undergoes the stress-free strains E^T_{11}, E^T_{22}, $-E^T_{12}$ so that mode I conditions prevail, as shown in Fig. 1. The explicit form of $\mathrm{d}K_{tip}$ has been reported by

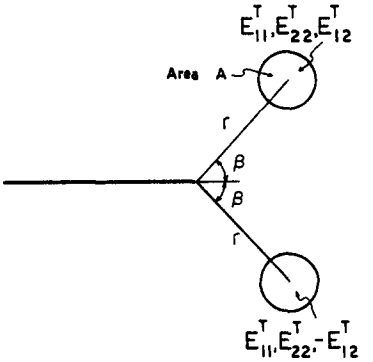

Fig. 1. Two symmetrically placed inclusions of circular cylindrical shape in the presence of a semi-infinite crack (mode I).

Hutchinson[21] and for infinitesimal dA it is given by

$$dK_{tip} = \frac{1}{\sqrt{(8\pi)}} \frac{E\,dA}{1-\nu^2} r^{-3/2} M(E^p_{\gamma\delta}, \beta), \tag{28}$$

where

$$M(E^p_{\gamma\delta}, \beta) = E^p_{\alpha\alpha} \cos\frac{3\beta}{2} + 3E^p_{12} \cos\frac{5\beta}{2} \sin\beta + \frac{3}{2}(E^p_{22} - E^p_{11}) \sin\beta \sin\frac{5\beta}{2}. \tag{29}$$

In the expressions above Greek indices take the values 1, 2 whereas Latin indices take the values 1, 2, 3.

The constitutive relations of Section 2 are valid for a three dimensional solid, while the analysis in this section is specialized to plane strain conditions. We easily show that the inelastic strains ε^p_{ij} in a 3-D material result in a set of in-plane inelastic strains $E^p_{\alpha\beta}$ given by

$$\begin{aligned} E^p_{11} &= \frac{1+\nu}{3}\varepsilon^p_{ii} - \nu e^p_{\mu\mu} + e^p_{11}, \\ E^p_{22} &= \frac{1+\nu}{3}\varepsilon^p_{ii} - \nu e^p_{\mu\mu} + e^p_{22}, \\ E^p_{12} &= e^p_{12}, \end{aligned} \tag{30}$$

when the plane strain conditions $\varepsilon_{i3} = 0$ are enforced. Thus, we note that in order to calculate ΔK_{tip} from eqn (27), we need to know the shape and extent of the transformed zone Ω as well as the inelastic strains $E^p_{\alpha\beta}$ (or, equivalently ε^p_{ij} from eqn (30)) within Ω.

In Sections 4 and 5 we will carry out the calculation outlined in this section for the cases of stationary and steadily growing cracks, respectively. We will further discuss the shape and orientation effects by considering spherical and thin oblate spheroidal particles separately.

4. SIF ENHANCEMENT FOR STATIONARY CRACK

Before proceeding we briefly present the results of Budiansky *et al.*[14] who neglected any shear effects and considered the case in which the transforming particles were allowed to undergo only a volumetric stress-free strain ε^T_{ii}. Their results are independent of particle shape and they further showed that for a stationary crack under monotonically increasing loading

$$K_{tip} = K_\infty \tag{31}$$

implying that there is no toughness enhancement. The same conclusion (under more restrictive assumptions) was reached by McMeeking and Evans[13] as well.

For a stationary crack under monotonically increasing loading the qualitative features of the near-tip region are shown schematically in Fig. 2(a). Denoting by c_0 the total volume concentration of particles that may transform, we observe that near the tip there is a region in which all particles have transformed ($c = c_0$) due to the high stresses. Next, there is a partially transformed region ($0 < c < c_0$) in the sense that some (but not all) of the particles are transformed and, finally, a region in which no transformation has occurred ($c = 0$). Figure 2(b) shows the same regions for the case in which all particles are identical. Near the tip we have a fully transformed region ($c = c_0$), whereas further out no transformation has taken place. The calculations to be reported in this section are valid for the case in which all particles within the transformed zone are actually transformed as shown in Fig. 2(b).

As the boundary of the transformed region Ω is approached from outside, no trans-

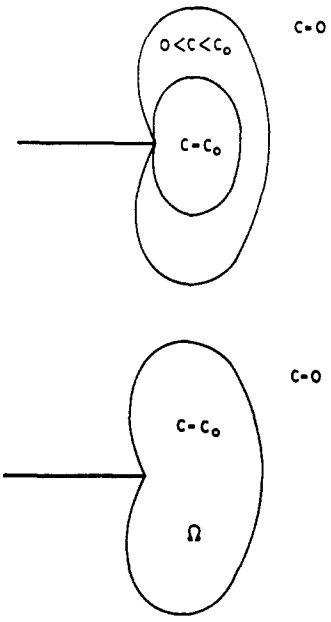

Fig. 2. Schematic representation of the transformed region for a stationary crack loaded monotonically: (a) some (but not all) particles transformed, (b) all particles transformed within the transformed region Ω.

formation has taken place and, hence, the average matrix stresses σ_{ij}^M are equal to the average overall stresses $\bar{\sigma}_{ij}$. Furthermore, we assume that the level of transformation (as measured by $c_0\varepsilon_{ii}^T$) within Ω is small enough so that the stress state as the boundary of Ω is approached from outside is approximately given by the unperturbed elastic solution, eqn (24). Thus, under monotonically increasing K_∞, we find the boundary $R(\theta)$ of Ω by using the critical transformation equation (4) and eqn (24), i.e.

$$F(\bar{\sigma}_{ij}) = H(c_0) \equiv A,$$
$$\bar{\sigma}_{ij} = \frac{K_\infty}{\sqrt{(2\pi R(\theta))}} f_{ij}(\theta). \tag{32}$$

$R(\theta)$ is found explicitly by eliminating σ_{ij} from the two equations above.

The 3-D inelastic strains are found by employing eqn (6) in the form

$$\varepsilon_{ij}^p = c_0 g_{ij}(\sigma^M) \tag{33}$$

and, finally, we relate the average $\bar{s}_{ij}$ and matrix s_{ij}^M deviatoric stresses on the boundary $R(\theta)$ of Ω by

$$\bar{s}_{ij} = (1-c_0)s_{ij}^M \tag{34}$$

as transformation takes place under vanishing s_{ij}^G within the particles as discussed in Section 2. The use of eqns (33) and (34) allows the complete determination of the 3-D inelastic strains ε_{ij}^p within Ω, and, hence, of the effective in-plane inelastic strains $E_{\alpha\beta}^p$ from eqn (30). Thus, we may evaluate ΔK_{tip} by the double integral of eqn (27).

For the case of spherical particles the function $F(\sigma_{ij})$ is given by eqn (19) and the 3-D inelastic strains are provided by eqns (23) where e_{ij}^T is given by (16) with s_{ij}^M evaluated on the boundary $R(\theta)$ of Ω. To show the results for ΔK_{tip} for spherical particles we denote the right-hand side of the first of eqns (32) by A_0; we evaluated ΔK_{tip} for the limiting cases of

small or large A_0. We found (for $\nu = 0.3$)

$$\frac{\Delta K_{tip}}{c_0 K_\infty} = -0.17 + qA_0 + O(A_0^2), \qquad A_0 \to 0,$$
$$\frac{\Delta K_{tip}}{c_0 K_\infty} = -0.09 \frac{1}{\sqrt{A_0}}, \qquad A_0 \to \infty, \tag{35}$$

where q is a positive number which has not been evaluated. The first of eqns (35) was derived analytically, whereas the second of (35) required a simple numerical integration. The effect in the SIF enhancement that is predicted by eqns (35) is very small as will be shown below.

We next discuss shape effects by studying the case where the transforming inclusions are thin oblate spheroids. It is obvious that we have to take into account orientation effects, i.e. the fact that due to their shape the particles have a given orientation with respect to the crack plane. We examine the influence of orientation on the SIF enhancement by assuming that all particles have the same orientation.

Three different orientations are considered as shown in Fig. 3 where they are labelled L_1, L_2 and L_3, respectively. Now the function F of eqn (32) is given by eqn (A1) of the Appendix and we identify the right-hand side in the first of (32) by A_1, A_2 and A_3 according as to whether the orientation is L_1, L_2 or L_3, respectively. The functions g_{ij} of eqn (6) are provided in eqn (A2) of the Appendix and, thus, ΔK_{tip} can be calculated by the double integral of eqn (27). The integral was evaluated numerically and the results for the orientations L_1, L_2 and L_3 are shown in Figs. 4, 5 and 6, respectively, where $\Delta K_{tip}/c_0 K_\infty$ is plotted as a function of A_1, A_2 or A_3 for two values of the aspect ratio λ of the particles.

From eqns (35) or from Figs. 4–6 we note that $\Delta K_{tip} < 0$ implying, from eqn (26), that $K_{tip} < K_\infty$. Thus, the effect of transformation is to relieve the stresses in the neighborhood of the crack-tip. Furthermore, by comparing Figs. 4–6 we observe that the effect of orientation L_1 is more beneficial than orientations L_2 and L_3. Lastly, we observe that ΔK_{tip} is maximized as $A_i \to 0$: As A_i is proportional to the level of critical stressing required for transformation, viz. eqn (32), we must exclude the limiting case of very small A_i as such particles will transform prior to the introduction of the crack.

To get an estimate of $\Delta K_{tip}/K_\infty$ we employ eqns (35) by using a typical value $c_0 = 0.3$. We get that $\Delta K_{tip}/K_\infty \cong -0.05$ for spherical particles. To estimate the effect of orientation L_1 we neglect the contributions of L_2 and L_3 (as they are much smaller than that of L_1) and we use Fig. 4 from where we get that the maximum contribution is $\Delta K_{tip}/c_0 K_\infty \cong -0.7$.

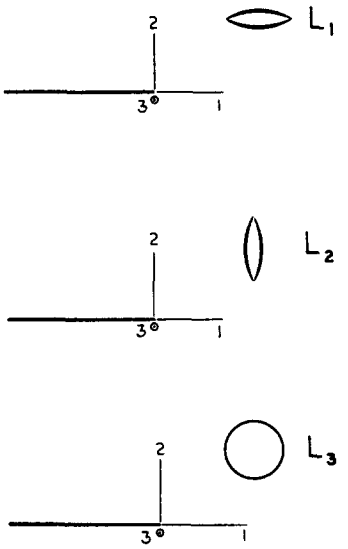

Fig. 3. Three possible orientations of an oblate spheroid with respect to the crack plane.

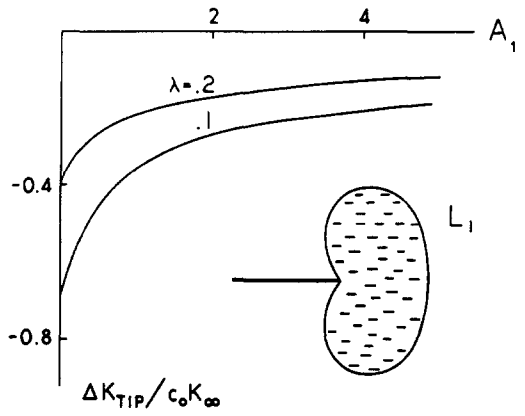

Fig. 4. SIF enhancement vs A_1 (orientation L_1) for a stationary crack.

Using a typical value for c_0, $c_0 = 0.1$ (as in reality equal amounts of each orientation are present[12]), we conclude that $\Delta K_{tip}/K_\infty = -0.07$. We conclude that whether the particles are spherical or equidistributed oblate spheroids, the effect of the transformation is to enhance the SIF but only by a very small amount which cannot account for the much larger increase in toughness measured in the laboratory[4, 5, 7, 12, 17].

5. TOUGHNESS ENHANCEMENT FOR STEADY-STATE QUASI-STATIC CRACK GROWTH

Having discussed the stationary crack, we proceed to consider the growing crack. We assume that the crack starts to grow and continues to grow quasi-statistically with K_{tip} maintained at a critical value. The applied SIF K_∞ increases with crack advance. For the case of uniform particles characterized by purely dilatational transformation, McMeeking and Evans[13] showed that the applied K_∞ increases with crack advance and that it approaches a constant steady-state value after a small amount of crack advance. In an actual toughness test the steady-state value of K_∞ is not reached because the crack will run unstably at a smaller value of the applied K_∞. However, the value of K_∞ at which the crack will grow unstably is expected to be close to the steady-state values as argued by Budiansky *et al.*[14]. Thus, calculation of the steady-state value provides the maximum possible toughness enhancement.

As the crack grows, it leaves behind it a wake of transformed particles. The height of the wake is denoted by H as shown in Fig. 7(a). Two different regions exist within the wake: A fully transformed region in which all the particles have transformed ($c = c_0$); and a partially transformed region in which some (but not all) of the particles have transformed. Loading takes place in the forward part of the transformed region as shown in Fig. 7(a). Figure 7(b) shows the same regions when all the particles are identical so that all particles

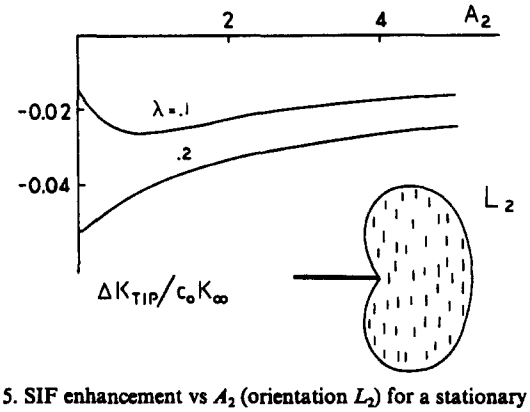

Fig. 5. SIF enhancement vs A_2 (orientation L_2) for a stationary crack.

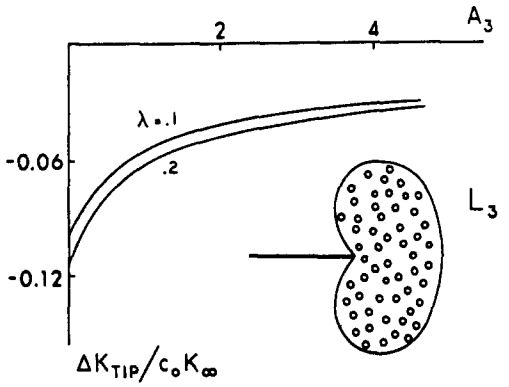

Fig. 6. SIF enhancement vs A_3 (orientation L_3) for a stationary crack.

are transformed within the transformed zone Ω. The results to be reported in this section are applicable to this last case.

Under the small scale transformation condition, the only relevant length scale is the height H of the wake as shown in Fig. 7. Thus, the stresses remote from the crack tip and outside the wake are given by eqn (24). Furthermore, the stresses are unchanged for an observer moving with the crack tip due to the steady-state assumption.

Before proceeding to use the constitutive relations of Section 2, we will review and present two special cases which are worth noting due to their simplicity. The first case corresponds to purely dilatational behavior (with $\varepsilon_{ii}^T \equiv \varepsilon^T$) and has been presented by McMeeking and Evans[13] and by Budiansky *et al.*[14]. The critical transformation condition is

$$\sigma_m = \sigma_0, \qquad (36)$$

$$\sigma_m = \tfrac{1}{3}\sigma_{ii},$$

where σ_0 is the (constant) magnitude of the mean stress required for transformation. Under these circumstances, the toughness enhancement can be easily found by the method of

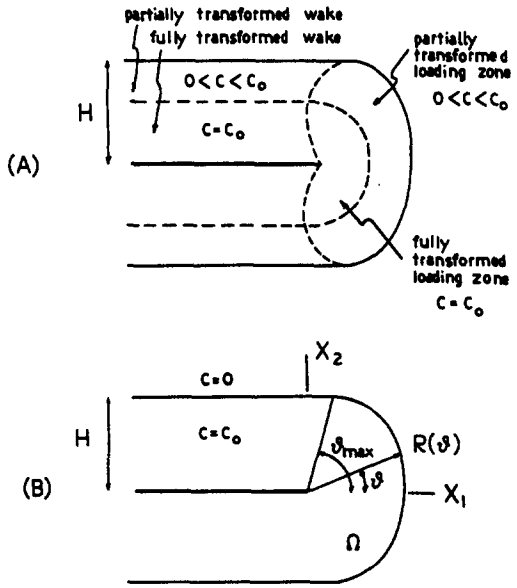

Fig. 7. Schematic representation of the transformed region for steady-state quasi-static crack growth: (a) some (but not all) particles transformed, (b) all particles transformed within the transformed region Ω.

Section 3 (see also[14]) as

$$\Delta K_{\text{tip}} = -0.214 \frac{E c_0 \varepsilon^T}{1-\nu} \sqrt{H}. \tag{37}$$

Another interesting special case is to consider spherical particles that will transform when the largest principal stress achieves a critical value σ_0. We assume that transformation is such that the only component of the transformation strain is ε^T in the direction of the largest principal stress[22]. We write the transformation criterion as

$$\max\{\sigma_{\text{I}}, \sigma_{\text{II}}, \sigma_{\text{III}}\} = \sigma_0, \tag{38}$$

where σ_{I}, σ_{II} and σ_{III} are the principal stresses. By using the unperturbed elastic solution for the stresses, eqn (24), we find the principal stresses as

$$\begin{Bmatrix} \sigma_{\text{I}} \\ \sigma_{\text{II}} \\ \sigma_{\text{III}} \end{Bmatrix} = \frac{K_\infty}{\sqrt{(2\pi r)}} \cos\frac{\theta}{2} \begin{Bmatrix} 1-\sin\dfrac{\theta}{2} \\ 1+\sin\dfrac{\theta}{2} \\ 2\nu \end{Bmatrix}.$$

Hence, the leading front $R(\theta)$ of the transformed region Ω is given by

$$\frac{K_\infty}{\sqrt{(2\pi R(\theta))}} \cos\frac{\theta}{2}\left(1+\sin\frac{\theta}{2}\right) = \sigma_0$$

or

$$2\pi\left(\frac{\sigma_0}{K_\infty}\right)^2 R(\theta) = \left[\cos\frac{\theta}{2}\left(1+\sin\frac{\theta}{2}\right)\right]^2. \tag{39a}$$

This expression is valid for $0 \leqslant \theta \leqslant \theta_{\max}$ where $\theta_{\max}$ is the angle at which the tangent to $R(\theta)$ becomes parallel to the crack growth direction; see Fig. 7(b). For $\theta_{\max} \leqslant \theta \leqslant \pi$ the boundary of Ω is given by

$$R(\theta) = \frac{H}{\sin\theta}, \tag{39b}$$

where H is the half-height of the transformed zone Ω. The shape of Ω, as given by eqns (39a) and (39b) is shown in Fig. 8, where we also show the dilatational contour of eqn (36) for purposes of comparison. From eqns (39a) and (39b) we easily find that the half-height H of the wake defined by

$$H \equiv R(\theta_{\max}) \sin\theta_{\max} \tag{40}$$

is given by

$$2\pi H\left(\frac{\sigma_0}{K_\infty}\right)^2 = 1.57 \tag{41}$$

and that $\theta_{\max}$ is equal to 74.8°.

The components of the transformation strain tensor in the coordinate system of the

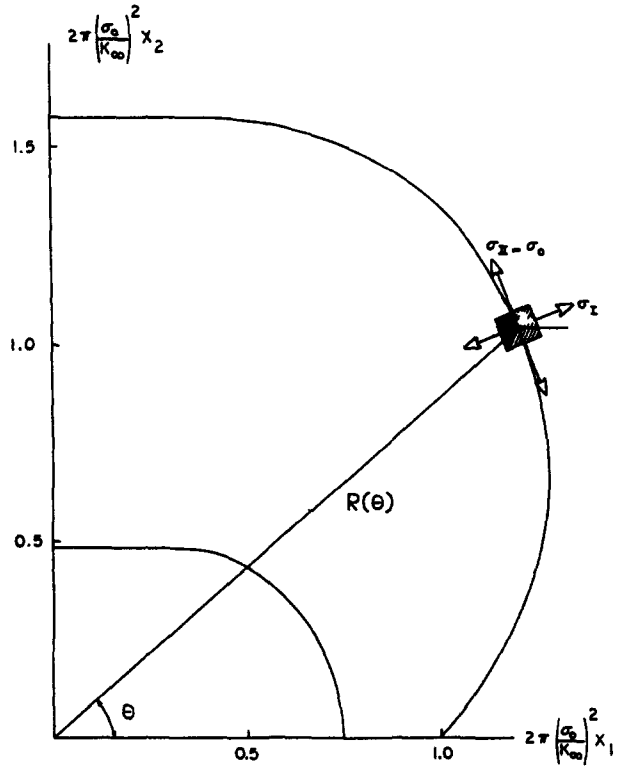

Fig. 8. Leading front of transformed region for steady-state quasi-static crack growth when transformation occurs at critical value σ_0 of maximum principal stress σ_{II}, eqn (38). For comparison, the dilatational contour of eqn (36) is also shown (dashed).

principal stress axes are written as

$$\begin{bmatrix} 0 & 0 & 0 \\ 0 & \varepsilon^T & 0 \\ 0 & 0 & 0 \end{bmatrix}. \tag{42}$$

Thus, we easily find the components of the transformation strain in the coordinate system of the crack as

$$\frac{\varepsilon^T}{2}\begin{bmatrix} 1-\sin\frac{3\theta}{2} & \cos\frac{3\theta}{2} & 0 \\ \cos\frac{3\theta}{2} & 1+\sin\frac{3\theta}{2} & 0 \\ 0 & 0 & 0 \end{bmatrix} \tag{43}$$

with the angle θ shown in Fig. 8. We note that as soon as a material particle crosses the leading front of Ω, it "picks up and freezes-in" the transformation strain which is constant in magnitude but changes in direction as the leading front $R(\theta)$ of Ω is spanned from $\theta = 0$ to $\theta = \theta_{max}$ (compare (42) and (43)). Thus, the transformation strain within Ω depends only on x_2 (Figs. 7(b) and 8).

The inelastic strains within the wake are found as

$$\varepsilon_{ij}^0 = c_0 \varepsilon_{ij}^T$$

and we can proceed to find the effective in-plane inelastic strains from eqns (30). Finally,

we calculate ΔK_{tip} by integrating numerically eqn (27) whose integrand is provided by eqns (28) and (29). We find

$$\Delta K_{tip} = -\frac{3.144}{4\pi}\frac{E}{1-\nu^2}\frac{K_\infty}{\sigma_0}c_0\varepsilon^T. \tag{44}$$

Equation (44) is not convenient to use as the magnitude of the critical stress σ_0 required for transformation is difficult to measure. However, we can eliminate σ_0 from eqns (41) and (44) to get

$$\Delta K_{tip} = -0.550Ec_0\varepsilon^T\sqrt{H}. \tag{45}$$

Comparing eqns (37) and (45) we observe that for a given value of the quantity $Ec_0\varepsilon^T\sqrt{H}$, transformation according to maximum principal stress, eqn (38), predicts toughness enhancement which is considerably in excess of the toughness enhancement predicted when transformation is according to mean stress, eqn (36).

Next, we briefly outline the way in which ΔK_{tip} can be calculated for the case of spherical particles. As in Section 4, we again assume that $c_0\varepsilon_{ii}^T$ is small enough so that the stresses, as the leading front of the transformed zone Ω is approached from outside, are approximately given by the unperturbed elastic solution, eqn (24). The leading front $R(\theta)$ of Ω is found by eliminating $\bar{\sigma}_{ij}$ from eqns (32) with $F(\bar{\sigma}_{ij})$ given by eqn (19) for the case of spherical particles. Thus, we find

$$\frac{2\pi p_0^2}{K_\infty^2}R(\theta) = w(\theta, A_0), \qquad 0 \leqslant \theta \leqslant \theta_{max}(A_0), \tag{46a}$$

where w is a dimensionless function of its arguments and θ_{max} is shown in Fig. 7(b). For $\theta_{max} \leqslant \theta \leqslant \pi$ the boundary of Ω is parallel to the crack growth direction and it is given by

$$R(\theta) = H/\sin\theta, \qquad \theta_{max} \leqslant \theta \leqslant \pi, \tag{46b}$$

where H is the half-height of the wake defined by eqn (41). Eliminating $R(\theta_{max})$ from eqns (46a) and (41) yields

$$\frac{2\pi p_0^2}{K_\infty^2}H = \delta(A_0), \tag{47}$$

δ being a dimensionless function of A_0.

To calculate the distribution of inelastic strains within Ω, we first observe that the inelastic dilatation is constant within Ω and equal to $c_0\varepsilon_{ii}^T$. Furthermore, the inelastic deviatoric strains within Ω are given by [see eqn (16)]

$$e_{ij}^p = c_0\frac{s_{ij}^M}{2G(1-\beta)},$$

where s_{ij}^M is the matrix deviatoric stress evaluated on the leading front $R(\theta)$ of Ω. Thus, the deviatoric inelastic strains within Ω depend only on x_2 [Fig. 7(b)]: The matrix stresses s_{ij}^M on $R(\theta)$ are related to the average deviatoric stresses $\bar{s}_{ij}$ by eqn (34) and, lastly, $\bar{s}_{ij}$ on $R(\theta)$ is given by

$$\bar{s}_{ij} = \bar{\sigma}_{ij} - \tfrac{1}{3}\bar{\sigma}_{kk}\delta_{ij},$$

$$\bar{\sigma}_{ij} = \frac{K_\infty}{\sqrt{(2\pi R(\theta))}}f_{ij}(\theta).$$

Having found ε_{ij}^{p} in the manner outlined above, we calculate the effective in-plane inelastic strains $E_{\alpha\beta}^{P}$ from eqns (30) and we evaluate the toughness enhancement ΔK_{tip} by numerical integration from eqn (27) with the integrand given by eqns (28) and (29).

The toughness enhancement is shown in two ways: First, by plotting K_{tip}/K_{∞} vs A_0^{-1} [Fig. 9(a)] or, by eliminating A_0 in favor of H by using eqn (47), by plotting $\Delta K_{tip}/K_{tip}$ vs $E\varepsilon_{ii}^{T}\sqrt{H}/K_{tip}$ [Fig. 9(b)]. Since the quantity A_0 is difficult to measure independently, a plot such as the one in Fig. 9(a) is not of direct use. However, we can draw interesting information by interpreting A_0^{-1} as equal to p_0/Σ_c, where Σ_c is a measure of the level of critical stressing required for transformation. Thus, we conclude from Fig. 9(a) that to maximize toughening we need to minimize Σ_c (however, we must still have Σ_c large enough to ensure stress-induced transformation). Rose[23] has further examined under what conditions on Σ_c K_{tip}/K_{∞} can be made to vanish for the case of purely dilatational transformation.

The results of Fig. 9(b), including the predictions of eqn (37) for purely volumetric stress-free strain labeled by "dilatation only", can be used if the height H of the transformed zone is known to predict ΔK_{tip}. Using typical values for the transformation parameters ($E = 200$ GPa, $\varepsilon_{ii}^{T} = 0.04$, $H = 4\times10^{-6}$ m, $K_{tip} = 4$ MPa$\sqrt{\text{m}}$) we see that the inclusion of shear effects gives $\Delta K_{tip}/K_{tip} \cong -0.5$ whereas pure dilatation predicts $\Delta K_{tip}/K_{tip} \cong -0.4$.

The same analysis can be carried out for thin oblate spheroidal particles when all particles are oriented along L_1, L_2 or L_3 (see Fig. 3): The corresponding results are shown in Figs. 10, 11 and 12, respectively, for several values of the aspect ratio λ of the particles. Figures 10(b), 11(b) and 12(b) also show the predictions of eqn (37) corresponding to purely volumetric stress-free strain labeled as "only ε_{ii}^{T}". We observe that the toughness enhance-

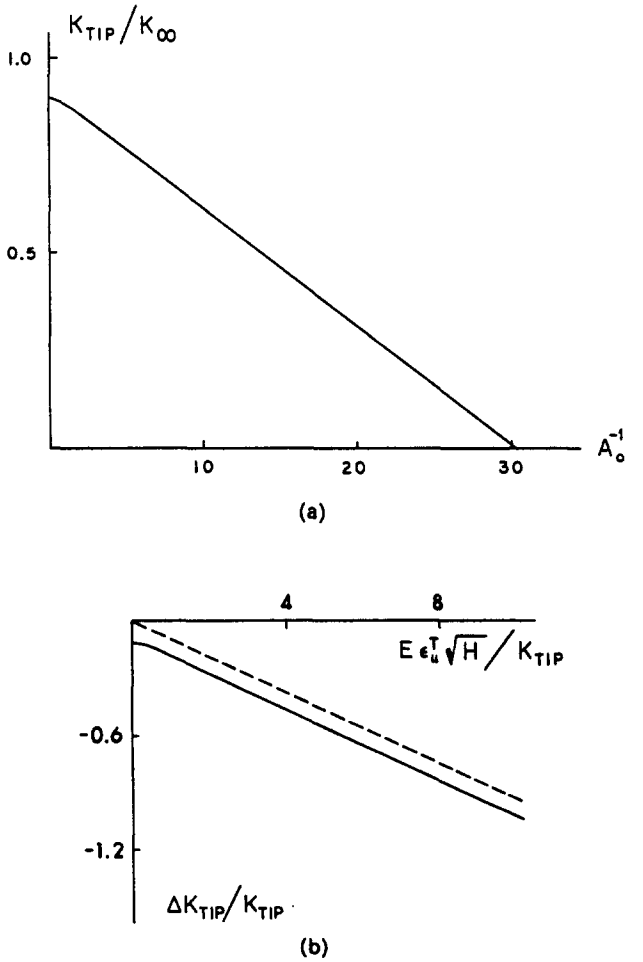

Fig. 9. Toughness enhancement by spherical particles ($\nu = c_0 = 0.3$): (a) K_{tip}/K_{∞} vs A_0^{-1}, (b) $\Delta K_{tip}/K_{tip}$ vs $E\varepsilon_{ii}^{T}\sqrt{H}/K_{tip}$. For comparison, the purely dilatational result is also shown[14].

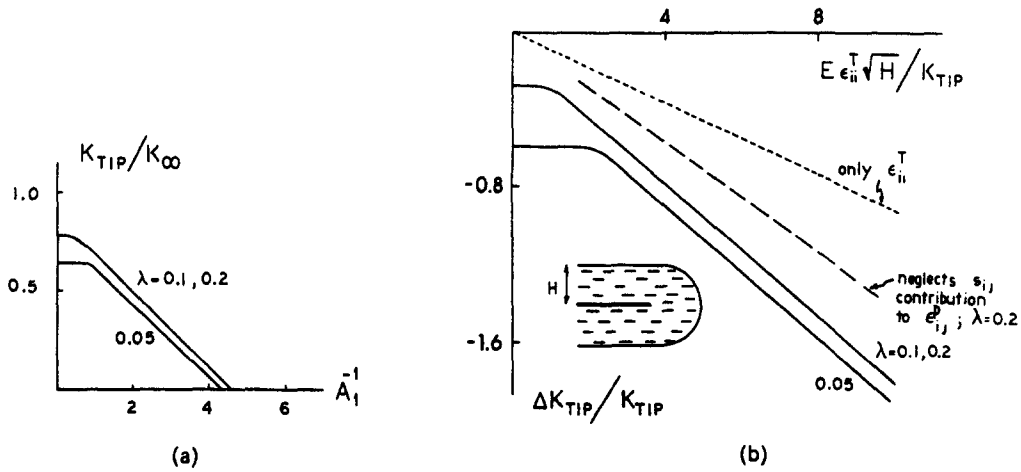

Fig. 10. Toughness enhancement by oblate spheroids (orientation L_1, $\nu = c_0 = 0.3$, aspect ratio λ): (a) K_{tip}/K_∞ vs A_1^{-1}, (b) $\Delta K_{tip}/K_{tip}$ vs $E\varepsilon_{ii}^T\sqrt{H}/K_{tip}$. For comparison, the purely dilatational result is also shown[14].

ment due to orientation L_1 is considerably greater than the toughness enhancement due to L_2 or L_3.

We end this section by considering the simplified form of the constitutive law applicable to thin oblate spheroids which is presented in eqns (A3) and (A4) of the Appendix. In the simplified constitutive law, the inelastic strains are constant within the wake. Thus, the

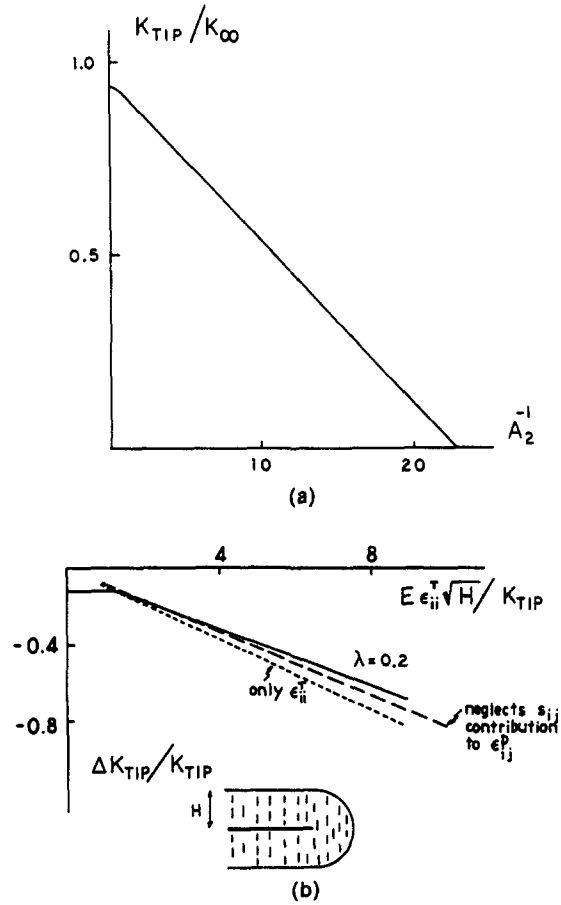

Fig. 11. Toughness enhancement by oblate spheroids (orientation L_2, $\nu = c_0 = 0.3$, aspect ratio $\lambda = 0.2$): (a) K_{tip}/K_∞ vs A_2^{-1}, (b) $\Delta K_{tip}/K_{tip}$ vs $E\varepsilon_{ii}^T\sqrt{H}/K_{tip}$. For comparison, the purely dilatational result is also shown[14].

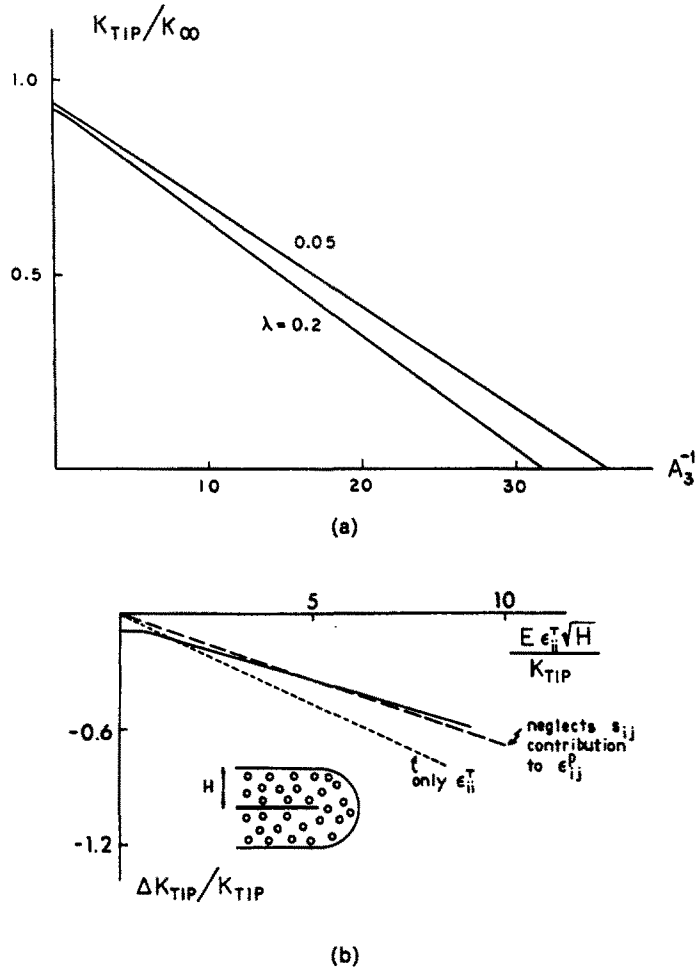

Fig. 12. Toughness enhancement by oblate spheroids (orientation L_3, $\nu = c_0 = 0.3$, aspect ratio λ): (a) K_{tip}/K_∞ vs A_3^{-1}, (b) $\Delta K_{tip}/K_{tip}$ vs $E\varepsilon_{ii}^T\sqrt{H}/K_{tip}$. For comparison, the purely dilatational result is also shown[14].

toughness enhancement can be found analytically rather than by numerical integration. The results of the use of the simplified constitutive law are shown in Figs. 10(b), 11(b) and 12(b) labeled by "neglects s_{ij} contribution to e_{ij}^p". From these figures we observe that the predictions of the simplified version are in reasonably good agreement with the predictions of the more involved constitutive law of eqns (A1) and (A2) of the Appendix. The agreement is better for orientations L_2 and L_3; the simplified version of the constitutive law for orientation L_1 underestimates the results of the more precise analysis presented earlier; see Fig. 10(b). However, due to its simplicity, we will use the simplified version in the next section in which we will discuss some experimental data.

6. DISCUSSION

There are several ceramic systems in which the transformation of ZrO_2 particles from tetragonal to monoclinic is used advantageously in order to enhance the fracture toughness of the composite ceramic. The two most widely studied ceramic systems where such transformation is exhibited are either partially stabilized zirconia (PSZ) within a cubic ZrO_2 matrix, or ZrO_2 particles within an Al_2O_3 matrix. Since the morphology of the ZrO_2 particles is dependent on the nature of the constraining matrix, these two systems will be discussed separately by using the results of Section 5.

Before proceeding, we pause to comment on the physical meaning of K_{tip} in the relation

$$K_{tip} = K_\infty + \Delta K_{tip}.$$

It has been shown[3, 8] that the toughness of a ceramic in which all ZrO_2 particles are transformed to monoclinic prior to the introduction of the crack is higher than the toughness of the material when no ZrO_2 particles are allowed to transform from tetragonal to monoclinic. The difference is attributed to the nature of the compressive stresses induced in the matrix due to the transformation which cause the subsequently introduced crack to deflect and bow out of its original plane. We account for the difference in toughness by identifying K_{tip} as the fracture toughness of the material when all the ZrO_2 particles are transformed to monoclinic prior to the introduction of the crack.

When the constraining matrix is Al_2O_3 the ZrO_2 particles are approximately spherical in shape[5, 17]. Since Young's modulus of Al_2O_3 is different from that of ZrO_3, we get an approximate value of the toughness enhancement by identifying E with the Young's modulus of the composite. Using $c_0 = 0.3$, $E = 315$ GPa [5], $\varepsilon_{ii}^T = 0.04$ [14], $H = 1 \times 10^{-6}$ m [5] and $K_{tip} = 5$ MPa$\sqrt{\text{m}}$ [5], we find

$$\frac{E\varepsilon_{ii}^T\sqrt{H}}{K_{tip}} = 2.5.$$

Thus, eqn (37) (purely volumetric transformation) predicts $\Delta K_{tip} = -1.2$ MPa$\sqrt{\text{m}}$, Fig. 9(b) (volumetric and shear stress-free strain) predicts $\Delta K_{tip} = -1.7$ MPa$\sqrt{\text{m}}$ and eqn (44) (transformation along maximum tensile axis) predicts $\Delta K_{tip} = -2.1$ MPa$\sqrt{\text{m}}$. The experimentally measured value is $\Delta K_{tip} = -2.4$ MPa$\sqrt{\text{m}}$ [5].

Another system of ZrO_2 particles within Al_2O_3 has $E = 470$ GPa, $c_0 = 0.3$, $\varepsilon_{ii}^T = 0.4$ and $H = 5 \times 10^{-6}$ m [14]. Equation (37) predicts $\Delta K_{tip} = -3.8$ MPa$\sqrt{\text{m}}$, Fig. 9(b) with $K_{tip} = 6$ MPa$\sqrt{\text{m}}$ yields $\Delta K_{tip} = -4.5$ MPa$\sqrt{\text{m}}$, whereas eqn (44) predicts $\Delta K_{tip} = -6.8$ MPa$\sqrt{\text{m}}$. The measure value is $\Delta K_{tip} = -6$ MPa$\sqrt{\text{m}}$ [14].

In the PSZ system the ZrO_2 particles are thin oblate spheroids oriented so that approximately one-third of the total volume concentration is along each of the principal planes of the cubic matrix[12]. It is observed that macroscopic cracks in such materials grow along the aforementioned principal planes. Thus, assuming that the total volume concentration of the ZrO_2 particles is $c_0 = 0.3$, particles of volume concentration $c_i = 0.1$ are along orientation L_i ($i = 1, 2, 3$) where the three orientations L_i with respect to the crack are shown in Fig. 3.

When all three orientations are present, the overall transformed region Ω is comprised of subregions Ω_i within which one, two or all three orientations have transformed. We study this mixture of orientations by employing the simplified constitutive law of eqns (A3) and (A4) of the Appendix. Furthermore, we assume that $c_0\varepsilon_{ii}^T$ is sufficiently small so that transformation within Ω_i does not alter the state of stress near the leading front $R_j(\theta)$ of Ω_j from the unperturbed elastic solution given by eqn (24). The use of the simplified version of the constitutive law in the form

$$\frac{1}{2}\frac{A_{22}}{A_{11}}\bar{s}_{33} + \bar{\sigma}_m = \sigma_0 = \text{constant}$$

allows the determination of the leading fronts $R_i(\theta)$ of the transformed subregions Ω_i. The different regions are shown in Fig. 13; the height of each wake is given by

$$H_i = \delta_i \frac{1}{2\pi}\left(\frac{K_\infty}{\sigma_0}\right)^2, \tag{48}$$

where $i = 1, 2, 3$ according as to whether the orientation of the particles is L_1, L_2 or L_3.

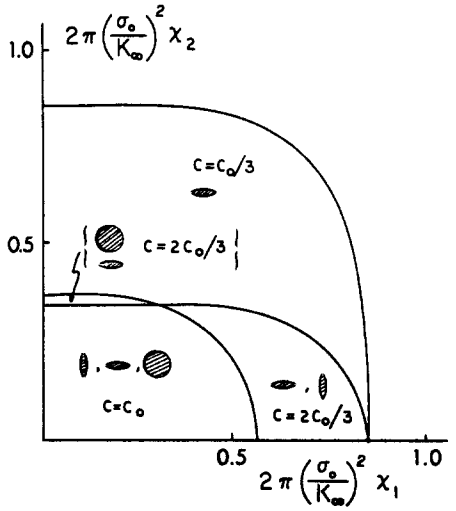

Fig. 13. Transformed region for steady-state quasi-static crack growth when all three orientations L_1, L_2 and L_3 are present. Results based on the simplified constitutive law for oblate spheroids.

The numerical values of the coefficients are

$$\delta_1 = 0.867, \qquad \delta_2 = 0.359, \qquad \delta_3 = 0.366.$$

The distribution of inelastic strains is constant within each Ω_i and it is given by eqn (A3) with dc replaced by c_0. The effective in-plane inelastic strains are found from eqns (30) and, thus, $\Delta K_{\text{tip}}^{(i)}$, the contribution to toughness due to orientation L_i within Ω_i, can be evaluated analytically from the double integral of eqn (27). We found

$$\Delta K_{\text{tip}}^{(i)} = -\beta_i E \varepsilon_{mm}^T c_i \frac{K_\infty}{\sigma_0} \qquad \text{(no sum on } i\text{)}$$

with

$$\beta_1 = 0.172, \qquad \beta_2 = 0.0651, \qquad \beta_3 = 0.0540$$

for $\nu = 0.3$ and for the aspect ratio $\lambda = 0.2$. The net toughness enhancement is

$$\Delta K_{\text{tip}} = \sum_{i=1}^{3} \Delta K_{\text{tip}}^{(i)}$$

which, upon elimination of σ_0 with the help of (48), is found as

$$\Delta K_{\text{tip}} = -0.082 E \varepsilon_{ii}^T \sqrt{H} \qquad (H \equiv H_1), \tag{49}$$

where we have identified H with H_1, the largest of the three heights H_i as can be seen from Fig. 13. Equation (49) is plotted together with eqn (37) in Fig. 14 for $\nu = 0.3$ and $c_0 = 0.3$. It is seen that the combination of the three orientations L_i predicts slightly lower toughness enhancement than the purely volumetric case. It must be borne in mind, however, that the contribution due to L_1 as found from the simplified constitutive law, eqns (A3) and (A4) of the Appendix, underestimated the more exact result (compare Fig. 10(b)). Thus, we conclude from Fig. 14 that a combination of all L_i yields essentially the same toughness enhancement as the purely volumetric case and, hence, the conclusions of Budiansky *et al.*[14] in comparing the predictions of eqn (37) with experimental data on PSZ are still valid: Equation (37) predicts that the value of the toughness enhancement is approximately one-third of the experimentally determined value.

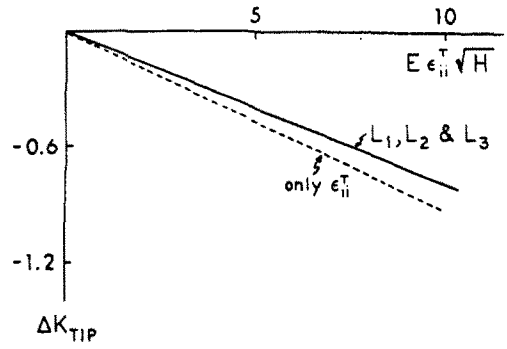

Fig. 14. Toughness enhancement ΔK_{tip} vs $E\varepsilon_{ii}^T H$ ($\nu = c_0 = 0.3$) for steady-state quasi-static crack growth as induced by the presence of all three orientations L_1, L_2 and L_3. For comparison, the purely dilatational result is also shown[14].

The agreement between theory and experiment may be brought closer if finite values of $c_0\varepsilon_{ii}^T$ are considered. Budiansky *et al.*[14] showed that the height of the transformed zone decreases compared to the unperturbed height as $c_0\varepsilon_{ii}^T$ increases. Thus, the value of H applicable in eqn (44) is not the actually measured height of the transformed zone but a larger number. A similar idea has been proposed by Evans and Heuer[1], who related the height H_T of the actual transformed zone to the height H_c of the unperturbed zone by

$$H_T = \eta(c_0)H_c. \tag{50}$$

Identifying H of (44) with H_c of (45), Swain *et al.*[7] showed that the experimentally found ΔK_{tip} correlates well with $\sqrt{H_T}$.

7. CONCLUSIONS

We have analyzed the effects of shear, shape and orientation in transformation toughening by proposing a continuum constitutive relation in the same spirit as metal plasticity by essentially "smearing out" the effect of transformed particles over the whole transformed region. We have shown that consideration of shear effects brings predicted values of toughness enhancement in good agreement with experimental results when the ZrO_2 particles are spherical. The agreement is not as good when oblate spheroidal particles are considered although we have identified an orientation that is decidedly more beneficial than the others.

We conclude by suggesting that further work is necessary to establish the validity of the continuum approach presented herein. The transformed zone may span from 3–5 to as many as 50 transformed particles and it is obvious that for the former case the continuum assumption may not be valid. It is also possible that a more careful analysis may be necessary of the mechanics of the shear band formation within the twinned transformed particles. However, we do believe that the present way of accounting for the shear in the particles is an effective approximation which should overestimate the effect of the shear component of the transformation. Given that the shear effect is predicted to be of secondary importance compared to the contribution of the dilatational transformation, the present approach may be adequate.

Acknowledgements—I wish to thank John Hutchinson who for the last two years has provided continued intellectual support and technical advice towards the completion of this work. Furthermore, I take this opportunity to thank various people (A. Evans, F. Rose, R. Cannon and J. Rice, among others) whose suggestions and ideas helped me in understanding transformation toughening. This work was supported in part by the National Science Foundation under Grant DMR-80-20247, and by the Division of Applied Sciences, Harvard University.

REFERENCES

1. A. G. Evans and A. H. Heuer, Review: Transformation toughening in ceramics: Martensitic transformations in crack-tip stress fields. *J. Am. Ceram. Soc.* **63**, 241–248 (1980).

2. R. C. Garvie, R. H. Hannink and R. T. Pascoe, Ceramic steel? *Nature* **258**, 703–704 (1975).
3. D. L. Porter and A. H. Heuer, Mechanisms of toughening partially stabilized zirconia (PSZ). *J. Am. Ceram. Soc.* **60**, 183–184 (1977).
4. T. K. Gupta, F. F. Lange and J. H. Bechtold, Effect of stress-induced phase transformation on the properties of polycrystalline zirconia containing metastable tetragonal phase. *J. Mater. Sci.* **13**, 1464–1470 (1978).
5. F. F. Lange, Transformation toughening, Parts 1–5. *J. Mater. Sci.* **17**, 225–262 (1982).
6. A. G. Evans, N. Burlingame, M. Drory and W. M. Kriven, Martensitic transformation in zirconia—particle size effects and toughening. *Acta Metall.* **29**, 447–456 (1981).
7. M. V. Swain, R. H. Hannink and R. C. Garvie, The influence of precipitate size and temperature on the fracture toughness of calcia- and magnesia-partially stabilized zirconia. In *Fracture Mechanics of Ceramics* (Edited by R. C. Bradt *et al.*), Vol. 6, pp. 339–382. Plenum Press, New York (1982).
8. H. Ruf and A. G. Evans, Toughening by monoclinic zirconia. *J. Am. Ceram. Soc.* **66**, 328–332 (1983).
9. W. M. Kriven, Martensite theory and twinning in composite zirconia ceramics. In *Advances in Ceramics* (Edited by A. Heuer and L. Hobbs), Vol. 3, pp. 168–183. American Ceramics Society (1981).
10. D. L. Porter, A. G. Evans and A. H. Heuer, Transformation-toughening in partially-stabilized zirconia (PSZ). *Acta Metall.* **27**, 1649–1654 (1979).
11. A. H. Heuer, Alloy design in partially stabilized zirconia. In *Advances in Ceramics* (Edited by A. Heuer and L. Hobbs), Vol. 3, pp. 98–115. American Ceramics Society (1981).
12. L. H. Schoenlein and A. H. Heuer, Transformation zones in Mg-PSZ. In *Fracture Mechanics of Ceramics* (Edited by R. C. Bradt *et al.*), Vol. 6, pp. 309–338. Plenum Press, New York (1982).
13. R. M. McMeeking and A. G. Evans, Mechanics of transformation toughening in brittle materials. *J. Am. Ceram. Soc.* **65**, 242–246 (1982).
14. B. Budiansky, J. W. Hutchinson and J. C. Lambropoulos, Continuum theory of dilatant transformation toughening in ceramics. *Int. J. Solids Structures* **19**, 337–355 (1983).
15. J. D. Eshelby, The determination of the elastic field of an ellipsoidal inclusion, and related problems. *Proc. R. Soc. London A* **241**, 376–396 (1957).
16. T. Mura, *Micromechanics of Defects in Solids*. Martinus Nijhoff, The Hague, The Netherlands (1982).
17. P. F. Becher and V. J. Tennery, Fracture toughness of Al_2O_3–ZrO_2 composites. In *Fracture Mechanics of Ceramics* (Edited by R. C. Bradt *et al.*), Vol. 6, pp. 383–398. Plenum Press, New York (1982).
18. G. K. Bansal and A. H. Heuer, On a martensitic phase transformation in zirconia, Part I. *Acta Metall.* **20**, 1281–1289 (1972); Part II, **22**, 409–417 (1974).
19. W. M. Kriven, W. L. Fraser and S. W. Kennedy, The martensite crystallography of tetragonal zirconia. In *Advances in Ceramics* (Edited by A. Heuer and L. Hobbs), Vol. 3, pp. 82–97. American Ceramics Society (1981).
20. J. R. Rice, Continuum mechanics and thermodynamics of plasticity in relation to microscale deformation mechanisms. In *Constitutive Equations in Plasticity* (Edited by Ali S. Argon), pp. 23–79. MIT Press, Cambridge, MA (1975).
21. J. W. Hutchinson, On steady quasi-static crack growth. Harvard University Report, Division of Applied Sciences, DEAP S-8 (April 1974).
22. R. Cannon, Verbal communication to J. Hutchinson (Spring 1984).
23. L. R. F. Rose, Theoretical aspects of transformation toughening, presented at the Eshelby Memorial Symposium, Sheffield, England, 2–5 April (1984).

APPENDIX

For the case of thin oblate spheroidal particles of semiaxes $a_1 = a_2 \gg a_3$, the function $F(\sigma_{ij}^M)$ is given by

$$F(\sigma_{ij}^M) = \frac{9(1-\nu)}{8(1+\nu)}\frac{1}{A_{11}}\left(\frac{s_{33}^M}{\tau_0}\right)^2 + \frac{1}{8}\frac{1}{A_{12}}\left|\left(\frac{s_{11}^M - s_{22}^M}{\tau_0}\right)^2 + 4\left(\frac{s_{12}^M}{\tau_0}\right)^2\right| + \frac{1}{2A_{33}}\left|\left(\frac{s_{13}^M}{\tau_0}\right)^2 + \left(\frac{s_{23}^M}{\tau_0}\right)^2\right| + \frac{\sigma_m^M}{\tau_0} + \frac{A_{22}}{A_{11}}\frac{s_{33}^M}{\tau_0} \tag{A1}$$

and the flow rule is

$$\begin{aligned}
\mathrm{d}e_{ii}^p &= \varepsilon_{ii}^T \mathrm{d}c,\\
\mathrm{d}(e_{11}^p - e_{22}^p) &= \frac{s_{11}^M - s_{22}^M}{2G}\frac{1}{A_{12}}\mathrm{d}c,\\
\mathrm{d}(e_{11}^p + e_{22}^p) &= -\left\{3\frac{1-\nu}{1+\nu}\frac{1}{A_{11}}\frac{s_{33}^M}{2G} + \frac{2}{3}\frac{A_{22}}{A_{11}}\varepsilon_{pp}^T\right\}\mathrm{d}c,\\
\mathrm{d}e_{12}^p &= \frac{s_{12}^M}{2G}\frac{1}{A_{12}}\mathrm{d}c,\\
\mathrm{d}e_{13}^p &= \frac{s_{13}^M}{2G}\frac{1}{A_{33}}\mathrm{d}c,\\
\mathrm{d}e_{23}^p &= \frac{s_{23}^M}{2G}\frac{1}{A_{33}}\mathrm{d}c,
\end{aligned} \tag{A2}$$

where

$$\tau_0 = G\varepsilon_{ii}^T$$

and

$$A_{11} = 1 - \frac{1+4\nu}{1+\nu}\frac{3\pi\lambda}{8}, \qquad A_{22} = 1 - \frac{3\pi\lambda}{4},$$

$$A_{12} = \frac{2-\nu}{1-\nu}\frac{\pi\lambda}{4}, \qquad A_{33} = \frac{2-\nu}{1-\nu}\frac{\pi\lambda}{4},$$

with λ being the aspect ratio $a_3/a_1 \ll 1$.

When the terms proportional to s_{ij}^M in eqn (14) or (A2) are dropped, the constitutive law is greatly simplified for the case of thin oblate spheroids; it becomes

$$F(\sigma_{ij}^M) = \frac{1}{2}\frac{A_{22}}{A_{11}}s_{33}^M + \sigma_m^M, \tag{A3}$$

$$\begin{aligned} \mathrm{d}\varepsilon_{ii}^p &= \varepsilon_{ii}^T \mathrm{d}c, \\ \mathrm{d}e_{11}^p = \mathrm{d}e_{22}^p &= -\frac{1}{3}\frac{A_{22}}{A_{11}}\varepsilon_{ii}^T \mathrm{d}c, \\ \mathrm{d}e_{33}^p &= \frac{2}{3}\frac{A_{22}}{A_{11}}\varepsilon_{ii}^T \mathrm{d}c, \\ \mathrm{d}e_{ij}^p &= 0 \qquad \text{for } i \neq j. \end{aligned} \tag{A4}$$